Applied Physics Letters ARTICLE scitation.org/journal/apl

Porous silicon nanowires phase transformations at high temperatures and pressures

Cite as: Appl. Phys. Lett. **119**, 053101 (2021); doi: 10.1063/5.0057706
Submitted: 24 May 2021 · Accepted: 19 July 2021 ·
Published Online: 2 August 2021

S. J. Rezvani,[1,a)] Y. Mijiti,[2] and A. Di Cicco[2,a)]

AFFILIATIONS

[1]Physics Division, School of Science and Technology, University of Camerino, 62032 Camerino, Italy and Advanced Materials Metrology and Life Science Division, INRiM (Istituto Nazionale di Ricerca Metrologica), Strada delle Cacce 91, Torino, Italy
[2]Physics Division, School of Science and Technology, University of Camerino, 62032 Camerino, Italy

[a)]**Authors to whom correspondence should be addressed:** sj.rezvani@unicam.it and andrea.dicicco@unicam.it

ABSTRACT

Porous silicon nanowires (NWs) with homogenous lateral dimensions of 90 nm are investigated by Raman scattering experiments along isothermal pressure cycles in a diamond anvil cell. Experiments were performed at variable temperatures up to 400 °C for maximal pressures of about 30 GPa comparing directly with transformations in bulk Si and porous NWs. Scanning electron microscopy demonstrates the persistence of one-dimensional morphology after high pressure investigation. The diamond phase in porous nanowires persists upon compression up to around 20 GPa at room temperature (25 °C) and to about 14 GPa at 200 °C and 400 °C. However, the $\beta-$Sn high pressure phase is seen to coexist with the diamond phase above 12 GPa at 25 °C and above 6 GPa at 200 °C and 400 °C. The coexistence region of the two phases is found to be considerably enlarged as compared with crystal silicon at each temperature. Upon decompression from 30 GPa, nucleation to the $\beta-$Sn, followed by formation of amorphous structures, is observed for porous NWs. Returning to ambient pressure and temperature, amorphous silicon is the dominant form with a residual contribution of $\beta-$Sn. At higher temperatures, nucleation back to the diamond structure is triggered although coexistence of amorphous and crystalline phases is observed up to 400 °C.

Semiconducting nanowires and, in particular, silicon nanowires (Si NWs) have been vastly studied and attracted the attention of an increasing audience of scientists as prototype materials for different applications as well as fundamental science.[1–6] Several methods have been suggested in recent decades for controlled fabrication of the nanowires that can result in distinct structural and electronic properties.[7–14] On the other hand, the modification of the electronic structure as a consequence of phase transitions occurring at high pressures and temperatures is well-known in bulk silicon, and at least 14 different stable and metastable phases have been observed, some of them showing exotic and promising properties for applications.[15–17] The behavior of silicon nanowires under high pressures and temperatures is much less studied, but several groups have already published papers in very recent times, discussing some of their properties under high pressures.[18–20] In those previous studies, the authors reported that the phase transitions' onsets in Si NWs are shifted to higher pressures as compared to bulk silicon, a fact that was mainly related to their sizes.[18,19] A very recent study was also carried out at higher temperatures (up to 165 °C), showing that at intermediate temperatures, substantial nucleation to an exotic low bandgap phase (bc8) was obtained in the recovered samples after a pressure cycle.[20]

In this work, we have carried out a systematic study of phase transitions in porous Si NWs (π-Si NWs) along isothermal pressure cycles extending up to 30 GPa and 400 °C by means of *in situ* Raman scattering experiments using an internally heated diamond anvil cell suitable for direct spectroscopic investigations.[21] The main aim is to investigate possible changes in phase transitions and nucleation of exotic phases at high pressures increasing temperatures, as compared to those of bulk silicon and crystalline Si NWs. Raman scattering was the technique of choice as it is also very sensitive to traces of crystalline forms. We have used well-characterized π-Si NWs of a typical lateral size of 90 nm that compares well with similar samples in previous studies. The nanowires investigated in this work were fabricated by metal assisted chemical etching using colloidal lithography that results in a uniform distribution of the NWs' lateral dimension. p-(B doped) type Si(100) substrates with a resistivity of 10–30 Ω cm were used for nanowire etching. The etching was carried out in a standard catalytic solution as indicated in detail in Ref. 10. The resulting wires have a

uniform outer diameter of the ∼90 nm and are ∼10 μm long. The wires have a random distribution of pore sizes ranging between 10 and 30 nm that results in a crystallite core to be of the order of 60–80 nm. The core crystallite has non-uniform shapes and can be separated or percolative[10,22] that makes their structure distinctive from the crystalline Si NWs with the single crystalline structure and the homogenous shape. Consequently, nanowires were scratched using the doctor blade technique and loaded into the anvil cell container.

Raman scattering experiments under high pressures and high temperatures have been performed using a micro-Raman setup equipped with an open-space confocal microscope Olympus BXFM with a suitable long-distance objective and optics collecting the Stokes portion of the Raman optical emission.

A properly filtered 50 mW green solid state laser was used as an excitation source ($\lambda = 532$ nm), focused in a sample area of about 5 μm, while Raman spectra were collected using a 1800 lines/mm grating by a scientific grade Peltier-cooled CCD covering a broad spectral range. Raman spectra were recorded in the 100–1100 cm^{-1} range with a 30 s of the acquisition time. The typical sample assembly inside the DAC space included well-characterized nanowires, a bulk B-doped crystal Si (c-Si) flake, and a $SrB_4O_7:Sm^{2+}$ chip as a pressure marker as shown in Fig. 1. The c-Si flake has been inserted in order to have a direct *in situ* monitoring of the phase transformations of a bulk system. The cell sample volume has been filled with NaCl as a pressure medium, previously successfully used in similar Raman experiments (see, for example, Ref. 23). The fluorescence lines of the samarium-doped strontium tetraborate ($SrB_4O_7:Sm^{2+}$) compound have been chosen as a pressure marker because of its better performance at high temperatures compared to the standard ruby technique.[24,25] High-pressure experiments were carried out at fixed temperatures corresponding to 25 °C, 100 °C, 200 °C, and 400 °C. The temperatures were accurately calibrated in advance[21] and measured *in situ* with a thermocouple and confirmed also via the shift of the c-Si Raman peaks.

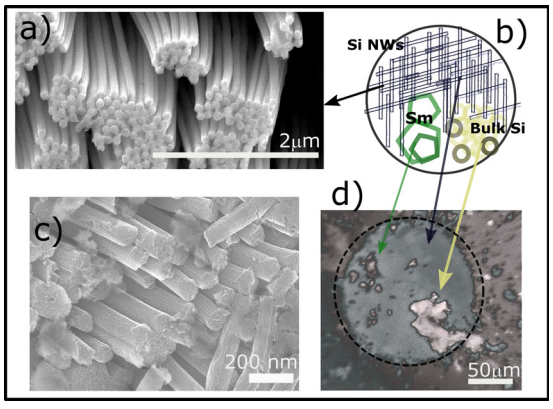

FIG. 1. (a) SEM image of the nanowires used in this investigation prior to loading. (b) Sketch of the sample assembly inside the gasket of the diamond anvil cell including the nanowires (Si NWs), bulk silicon (bulk Si), and $SrB_4O_7:Sm^{2+}$ (Sm) pieces. (c) SEM image of the Si nanowires after the compression/decompression cycles at ambient temperature. (d) Optical microscope image of the loaded gasket at 5 GPa showing the different components of the sample assembly inside the cell.

Selected *in situ* Raman spectra of bulk crystalline silicon (c-Si) and π-Si-NWs collected for individual isothermal compression–decompressioncycles at 25 °C, 200 °C, and 400 °C are shown in Fig. 2. It is useful to discuss first the compression phase (shown in the first three panels from left to right in Fig. 2) comparing what happens in c-Si and π-Si-NWs systems.

As it is known, for the diamond structure of c-Si (dc-Si, Si-I), there is a main transverse optical band (TO) at ∼521 cm^{-1} and a weak component at lower wavenumbers (∼285 cm^{-1}) assigned to the transverse acoustic phonons (2TA). The trend observed for c-Si (lower panels of Fig. 2) is in agreement with previous observations with the shift of TO modes of the dc-Si structure (Si-I) to higher wave numbers and the transformation to the β-Sn/Imma (Si-II/Si-XI) high-pressure phases as indicated in figure. Weak Raman components at ∼400 and ∼110 cm^{-1} are assigned to the β-Sn structure while another component at ∼270 cm^{-1} is usually assigned to the *Imma* one (overlapping the 2TA modes of Si-I).[26]

Coexistence of Si-I and Si-II phases is observed in a quite extended range 10–16 GPa, slightly reduced in pressure by increasing the temperature up to 400°. These findings are in excellent agreement with previously reported values for B-doped bulk silicon, slightly higher than that of intrinsic bulk silicon.[27] At higher pressures, corresponding to the nucleation to the hexagonal phase *sh*-Si (Si-V), the Raman signal is suppressed (the absence of active optical phonons and metallization).

The π-Si-NWs' Raman spectra reported in the upper panels of Fig. 2 show a TO mode shift toward lower wavenumbers (∼519 cm^{-1}) at ambient pressures and temperatures (not shown in figure) while having an asymmetric broadening due to the small crystallite lateral sizes within the nanowire.[28] Upon pressure increase, increasing pressures, the shift of the TO peak to higher wavenumber is clearly visible with the phase transitions to the β-Sn/Imma and to the *sh*-Si (Si-V) phase observed in a large range of pressures extended to ∼20 GPa. In π-Si-NWs samples, the observed transition pressures at room temperature are higher than that of c-Si with larger coexistence regions of the different phases. Higher and broader transition onsets in the porous nano-structure could be related to the presence of smaller crystallites within the pores as well as their non-homogenous shape distribution.[29] Similarly to c-Si, for increasing temperatures, a significative reduction of the transition pressures to the high-pressure phases is obtained. Pressures as low as ∼7 GPa are observed for nucleation to the Si-II phase.

The trend of selected Raman spectra collected on isothermal decompression from about 23 GPa is shown in Fig. 2, right-hand panels. Striking differences are observed at different temperatures.

For c-Si at room temperature, nucleation of the β-Sn/Imma (Si-II, Si-XI) phase occurs below 17 GPa, while crystallization to the r8/bc8 metastable phase is clearly observed below 10 GPa and retained down to ambient pressure. At higher temperatures (200 °C, 400 °C), c-Si shows different phase transformations upon decompression. The β-Sn/Imma (Si-II,Si-XI) phase formation is observable around 14 GPa, followed by nucleation to the dc-Si (Si-I), which is the dominant phase below 6 GPa. A mixture of Si-I and r8/bc8 phases is observed at 100 °C returning to ambient pressure (see Fig. 3).

The π-Si-NWs' Raman spectra on depressurization reported in the upper-right panels of Fig. 2 show a quite different behavior as compared to c-Si. Nucleation to the β-Sn/Imma (Si-II,Si-XI) phase occurs at considerably lower pressures (10, 13.5, and 15.4 GPa at

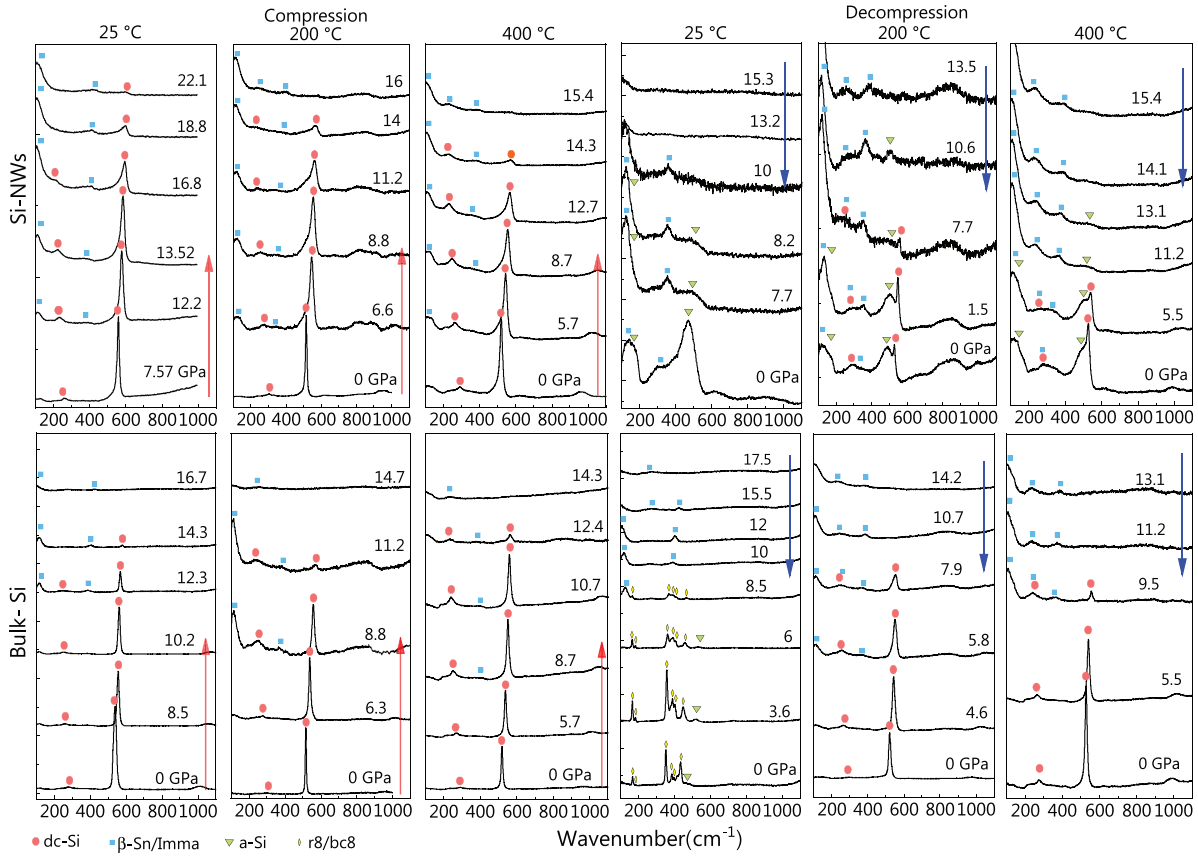

FIG. 2. Raman spectra of porous silicon nanowires (π-Si-NWs, upper panels) and bulk silicon (bulk-Si, lower panels) collected *in situ* for increasing (compression, first three columns) and decreasing pressures (decompression, see arrows). The isothermal pressure cycles were performed at different temperatures (25 °C, 200 °C, and 400 °C) shown from left to right for the compression and decompression stages.

25 °C, 200 °C, and 400 °C, respectively). Upon further decreasing the pressure below 10 GPa, nucleation to a tetrahedrally coordinated low-density amorphous (LDA, a-Si) phase is clearly observed. This is the dominant structure obtained releasing the pressure at room temperature, but at larger temperatures, partial nucleation to the diamond structure dc-Si (Si-I) is observed. Recent results[20] reported the evidence of the coexistence of r8/bc8 and a-Si (LDA) phases in single crystalline nanowires of typical 80–150 nm size (diameters) at temperatures below 165 °C upon decompression. We performed our isothermal Raman experiment under pressure also at 100 °C, and we did not observe the formation of this phase in π-Si-NWs, as shown in Fig. 3. Full results obtained at this temperature are not reported here for the sake of brevity but are in line with those shown in Fig. 2. Our observations indicate that the temperature increase favors nucleation to the dc-Si (Si-I) diamond phase at ambient pressures for both c-Si and π-Si NWs.

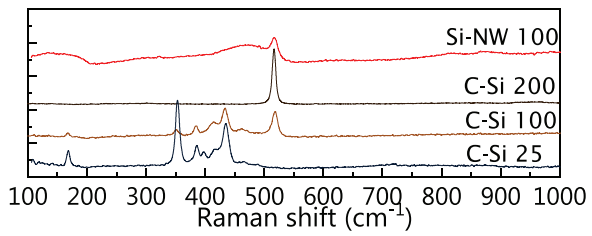

FIG. 3. Raman spectra of fully decompressed (after a compression cycle) c-Si at different temperatures of 25 (bc8/r8), 100 (mixture of bc8/r8 and Si-I), and 200 °C (Si-I) in comparison with π-Si NWs at 100 °C (a mixture of amorphous and Si-I).

Finally, in Fig. 4, the phase transitions observed in π-Si NWs are directly visualized on the c-Si phase diagram. Our results are also compared with literature data available for c-Si and single crystalline Si NWs. The initial transition from Si-I to Si-II is indicated by the empty circles and dashed lines in Fig. 4, and the shaded regions indicate our observations of the Si-II phase for both c-Si and π-Si NWs (blue). The results obtained for c-Si are in good agreement with previous observations,[27,31] although extended now to higher temperatures.

On the other hand, present results on porous nanowires' π-Si NWs indicate that typical phase transformations take place in a wider pressure interval as compared with previous results on crystalline Si-NWs,[18,20] as also shown in Fig. 4. The Raman data collected during the isothermal cycle at high pressures show that phase transformations are dramatically modified by the temperature. The peculiar behavior of π-Si NWs is illustrated in Fig. 4, lower panel, where the various

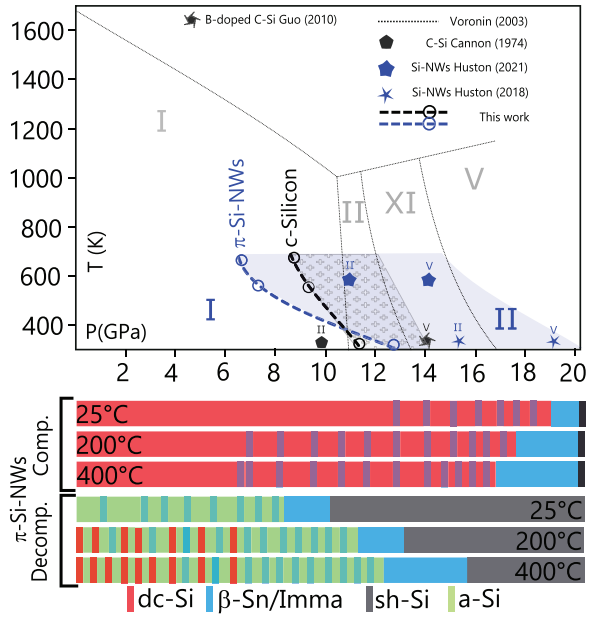

FIG. 4. Top: proposed silicon phase diagram based on Ref. 30, compared with the results (compression) of the present work and previously reported results.[18,20,27,31] Empty circles joined by dashed lines indicate present observations for the nucleation onsets to the Si-II phase, observed in the dashed-filled areas. Bottom: diagram showing phase transitions to different structures (shown in color) observed for porous nanowires (π-Si NWs) along compression/decompression cycles at selected temperatures.

structures observed under different thermodynamical conditions are shown. In particular, the porous nanowires can show a coexistence of covalent amorphous (LDA, a-Si), metallic β-Sn (Si-II), and semiconductor diamond (Si-I) structures when pressure is released.

In conclusion, our results indicate a large band of phase transition pressures in π-Si NWs. This peculiar behavior can probably be associated with a non-homogeneous size and shape distribution of porous nanowires as opposed to the crystalline nanowires with the single crystalline structure and relatively homogenous crystallite shape. The π-Si NWs, additionally, exhibit a distinct temperature dependence as compared with bulk c-Si and other crystalline Si-NWs. Upon releasing the pressure, π-Si NWs result in a combination of amorphous (LDA, a-Si) and $\beta-$Sn (Si-II) structures at room temperature with an increasing diamond (Si-I) structure content at higher temperatures. This behavior is very different from that of c-Si and to previous results obtained for crystalline NWs indicating the formation of the bc8 metastable phase.[20]

Our results on the porous NWs' structures of silicon clearly evidence that phase transitions either in compression or decompression are significantly affected by the initial structure of the materials especially at low dimension. Furthermore, our results at high temperatures demonstrate the possibility to achieve the distinct exotic phases in a much wider range of the temperatures and pressures compared with the crystalline structures. This variety of exotic phase transitions with distinct properties in porous Si nanowires can lead to advanced applications in the future. However, these results indicate that systematic studies are still required to better understand the mechanisms of the phase transition in such structures.

Y.M. thanks to the postdoc grant of the CRUI foundation. We thank Sergey V. Rashchenko at the Sobolev Institute of Geology and Mineralogy for providing Sm:SrB_4O_7 pressure calibrants.

DATA AVAILABILITY

The data that support the findings of this study are available from the corresponding author upon reasonable request.

REFERENCES

[1]L. T. Canham, Appl. Phys. Lett. **57**, 1046 (1990).
[2]Z. Kang, C. Tsang, N. Wong, Z. Zhang, and S. Lee, J. Am. Chem. Soc. **129**, 12090 (2007).
[3]L. Pavesi, L. Dal Negro, C. Mazzoleni, G. Franzo, and F. Priolo, Nature **408**, 440 (2000).
[4]A. Loni, T. Defforge, E. Caffull, G. Gautier, and L. Canham, "Porous silicon fabrication by anodisation: Progress towards the realisation of layers and powders with high surface area and micropore content," Microporous Mesoporous Mater. **213**, 188 (2015).
[5]M. T. Deng, C. L. Yu, G. Y. Huang, M. Larsson, P. Caroff, and H. Q. Xu, "Anomalous zero-bias conductance peak in a Nb-InSb nanowire-Nb hybrid device," Nano Lett. **12**, 6414 (2012).
[6]H. A. Nilsson, P. Samuelsson, P. Caroff, and H. Q. Xu, "Supercurrent and multiple andreev reflections in an InSb nanowire Josephson junction," Nano Lett. **12**, 228 (2012).
[7]S. J. Rezvani, L. Favre, G. Giuli, Y. Wubulikasimu, I. Berbezier, A. Marcelli, L. Boarino, and N. Pinto, "Spontaneous shape transition of Mn_xGe_{1-x} islands to long nanowires," Beilstein J. Nanotechnol. **12**, 366 (2021).
[8]R. S. Wagner and W. C. Ellis, "Vapor-liquid-solid mechanism of single crystal growth," Appl. Phys. Lett. **4**, 89 (1964).
[9]N. Pinto, S. J. Rezvani, L. Favre, I. Berbezier, M. Fretto, and L. Boarino, "Geometrically induced electron-electron interaction in semiconductor nanowires," Appl. Phys. Lett. **109**, 123101 (2016).
[10]S. J. Rezvani, R. Gunnella, D. Neilson, L. Boarino, L. Croin, G. Aprile, M. Fretto, P. Rizzi, D. Antonioli, and N. Pinto, "Effect of carrier tunneling on the structure of Si nanowires fabricated by metal assisted etching," Nanotechnology **27**, 345301 (2016).
[11]S. J. Rezvani, N. Pinto, and L. Boarino, "Rapid formation of single crystalline Ge nanowires by anodic metal assisted etching," CrystEngComm **18**, 7843 (2016).
[12]S. J. Rezvani, D. D. Gioacchino, C. Gatti, C. Ligi, M. C. Guidi, S. Cibella, M. Fretto, N. Poccia, S. Lupi, and A. Marcelli, "Proximity array device: A novel photon detector working in long wavelengths," Condens. Matter **5**, 33 (2020).
[13]S. J. Rezvani, N. Pinto, L. Boarino, F. Celegato, L. Favre, and I. Berbezier, "Diffusion induced effects on geometry of Ge nanowires," Nanoscale **6**, 7469 (2014).
[14]S. J. Rezvani, L. Favre, F. Celegato, L. Boarino, I. Berbezier, and N. Pinto, "Supersaturation state effect in diffusion induced Ge nanowires growth at high temperatures," J. Cryst. Growth **436**, 51 (2016).
[15]J. Crain, G. J. Ackland, and S. J. Clark, "Exotic structures of tetrahedral semiconductors," Rep. Prog. Phys. **58**, 705 (1995).
[16]A. Mujica, A. Rubio, A. Muñoz, and R. J. Needs, "High-pressure phases of group-iv, iii–v, and ii–vi compounds," Rev. Mod. Phys. **75**, 863 (2003).
[17]B. Haberl, T. A. Strobel, and J. E. Bradby, "Pathways to exotic metastable silicon allotropes," Appl. Phys. Rev. **3**, 040808 (2016).
[18]L. Q. Huston, A. Lugstein, J. S. Williams, and J. E. Bradby, "The high pressure phase transformation behavior of silicon nanowires," Appl. Phys. Lett. **113**, 123103 (2018).
[19]Y. Xuan, L. Tan, B. Cheng, F. Zhang, X. Chen, M. Ge, Q. Zeng, and Z. Zeng, "Pressure-induced phase transitions in nanostructured silicon," J. Phys. Chem. C **124**, 27089 (2020).
[20]L. Q. Huston, A. Lugstein, G. Shen, D. A. Cullen, B. Haberl, J. S. Williams, and J. E. Bradby, "Synthesis of novel phases in Si nanowires using diamond anvil cells at high pressures and temperatures," Nano Lett. **21**(0), 1427 (2021).
[21]Y. Mijiti, M. Perri, J. Coquet, L. Nataf, M. Minicucci, A. Trapananti, T. Irifune, F. Baudelet, and A. Di Cicco, "A new internally heated diamond anvil cell system for time-resolved optical and x-ray measurements," Rev. Sci. Instrum. **91**, 085114 (2020).

[22]S. J. Rezvani, N. Pinto, E. Enrico, L. D'Ortenzi, A. Chiodoni, and L. Boarino, "Thermally activated tunneling in porous silicon nanowires with embedded Si quantum dots," J. Phys. D: Appl. Phys. **49**, 105104 (2016).
[23]F. Coppari, J. Chervin, A. Congeduti, M. Lazzeri, A. Polian, E. Principi, and A. D. Cicco, "Pressure-induced phase transitions in amorphous and metastable crystalline germanium by Raman scattering, x-ray spectroscopy, and *ab initio* calculations," Phys. Rev. B **80**, 115213 (2009).
[24]S. V. Raju, J. M. Zaug, B. Chen, J. Yan, J. W. Knight, R. Jeanloz, and S. M. Clark, "Determination of the variation of the fluorescence line positions of ruby, strontium tetraborate, alexandrite, and samarium-doped yttrium aluminum garnet with pressure and temperature," J. Appl. Phys. **110**, 023521 (2011).
[25]A. V. Romanenko, S. V. Rashchenko, A. Kurnosov, L. Dubrovinsky, S. V. Goryainov, A. Y. Likhacheva, and K. D. Litasov, "Single-standard method for simultaneous pressure and temperature estimation using Sm^{2+}:SrB_4O_7 fluorescence," J. Appl. Phys. **124**, 165902 (2018).
[26]N. N. Ovsyuk and S. G. Lyapin, "Raman spectra of Si nanocrystals under high pressure: Metallization and solid state amorphization," Appl. Phys. Lett. **116**, 062103 (2020).
[27]J. J. Guo, D. Pan, X. Q. Yan, T. Fujita, and M. W. Chen, "Effect of doping and counterdoping on high-pressure phase transitions of silicon," Appl. Phys. Lett. **96**, 251910 (2010).
[28]K. W. Adu, H. R. Gutiérrez, U. J. Kim, G. U. Sumanasekera, and P. C. Eklund, "Confined phonons in Si nanowires," Nano Lett. **5**, 409–15755085 (2005).
[29]S. H. Tolbert, A. B. Herhold, L. E. Brus, and A. P. Alivisatos, "Pressure-induced structural transformations in Si nanocrystals: Surface and shape effects," Phys. Rev. Lett. **76**, 4384 (1996).
[30]G. A. Voronin, C. Pantea, T. W. Zerda, L. Wang, and Y. Zhao, "*In situ* x-ray diffraction study of silicon at pressures up to 15.5 GPa and temperatures up to 1073 K," Phys. Rev. B **68**, 020102 (2003).
[31]J. F. Cannon, "Behavior of the elements at high pressures," J. Phys. Chem. Ref. Data **3**, 781 (1974).